An asymmetrically side-coupled Sagnac-loop system with diverse mode splitting properties

Xinhong Jiang, Jiayang Wu, Liang Zhang, Xiaofeng Hu, Pan Cao, Xiaowen Sun, Xi Yin, and Yikai Su

State Key Laboratory of Advanced Optical Communication Systems and Networks, Department of Electronic Engineering, Shanghai Jiao Tong University, Shanghai 200240, China, E-mail: yikaisu@sjtu.edu.cn

Abstract — **We propose and experimentally demonstrate an asymmetrically side-coupled Sagnac-loop system on a silicon-on-insulator (SOI) platform. Diverse mode-splitting properties are obtained, with various transparency peaks between split resonances and high-order filtering function.**

Keywords — **mode splitting, microring resonators (MRRs), silicon-on-insulator (SOI).**

I. Introduction

Mode splitting of microring resonators (MRRs) has been used for various applications in recent years, such as dense wavelength conversion [1], fast/slow light [2, 3], and optical filtering [4]. MRR system with clockwise (CW) and counter-clockwise (CCW) degenerate resonance modes can be employed to generate mode splitting. Coupling between the CW and the CCW modes enabled by fabrication-induced sidewall roughness has been studied in Ref. [5], but it was difficult to control the mode splitting degree due to fabrication imperfections. Another scheme based on coupling between counter-propagation modes has been proposed in Ref. [6], which was realized by self-coupled optical waveguides (SCOWs). However, due to the symmetry of the configuration, only split resonances with identical spectral responses can be achieved with these devices.

In this paper, mode splitting with diverse transmission intensities is achieved by using asymmetrically side-coupled Sagnac loops consisting of two asymmetric Sagnac loops and a connecting bus waveguide. The mode-splitting transmission spectrum provides versatile intensity response that can be tailored with transmission coefficients, which is demonstrated by the measured transmission spectra of the fabricated devices. The proposed configuration could find applications in signal processing at various wavelengths. Furthermore, high-order filtering can also be obtained at some non-splitting resonances.

II. Device Structure and Operation Principle

Figure 1 illustrates the schematic of the proposed configuration. Two Sagnac loops are connected by Coupler 2 in the center. A bus waveguide is side-coupled to the bottom of the two Sagnac loops, which forms a Mach-Zehnder interferometer (MZI). R_1 and R_2 are the radii of the inner and outer bends, respectively. L_{c1}, L_{c2}, and L_{c3} are the coupling lengths of the three couplers. $L_a = 2R_1 + L_{c1}$ and $L_b = 4R_1 + L_{c2}$ are the lengths of the straight waveguides. The transmission coefficients of the three couplers are r_i ($i = 1, 2, 3$), respectively.

Coupling between counter-propagation modes is introduced by Coupler 2, leading to mode splitting in the proposed configuration. Since there is a difference between the lengths of the two waveguides connecting Coupler 1 (or 3) and Coupler 2, i.e., the Sagnac loops are asymmetrically coupled to
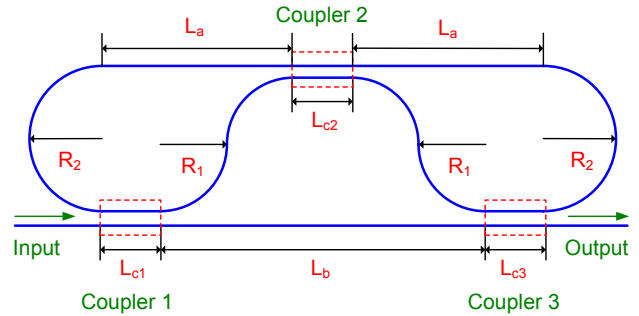

Fig. 1. Schematic of the proposed configuration.

the bus waveguide, transparency peaks between the split resonances in the transmission spectrum exhibit diverse transmission intensities.

Figure 2 shows the simulated transmission spectra of the proposed device with various transmission coefficients of the three couplers, which can be realized by changing the coupling lengths. The transmission spectra are calculated using the scattering matrix method [7]. The structural parameters are chosen as follows: $R_1 = 9.7$ μm, $R_2 = 10$ μm, waveguide width of 0.45 μm, and gap size of 0.18 μm due to fabrication limitation. It is assumed that the propagation loss of the waveguide is $\alpha \approx 6.5$ dB/cm and the waveguide group index of the transverse electric (TE) mode is $n_g \approx 4.3$ based on our previously fabricated devices. Diverse transmission intensities in the transparency peaks between the split resonances are evenly spaced in the transmission spectra. These differences in
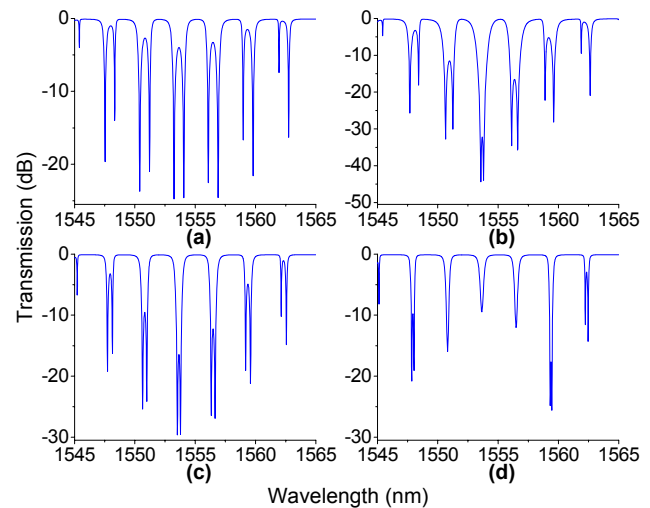

Fig. 2. Transmission spectra of the proposed configuration with various transmission coefficients of the three couplers. (a) $r_1 = r_3 = 0.9$, $r_2 = 0.9$. (b) $r_1 = r_3 = 0.8$, $r_2 = 0.9$. (c) $r_1 = r_3 = 0.9$, $r_2 = 0.97$. (d) $r_1 = r_3 = 0.9$, $r_2 = 0.99$.

transmission intensities are caused by the asymmetry of the two Sagnac loops, which provide richer spectrum than that in Ref. [6] with equal split resonances. From Fig. 2(a)-(c), one can see that the maximum transmission-intensity difference becomes larger with decreased r_1 and r_3 or increased r_2. Meanwhile, the separation between the two notches of a split resonance decreases. If r_2 becomes large enough, some mode-splitting resonances degenerate into non-splitting resonances with enlarged bandwidths, as shown in Fig. 2(d).

III. DEVICE FABRICATION AND MEASURED SPECTRA

The proposed device is fabricated on an 8-inch SOI wafer with a 220-nm-thick top silicon layer and a 2-μm-thick buried dioxide layer. The device layout is defined with 248-nm deep ultra-violet (DUV) photolithography followed by an inductively coupled plasma (ICP) etching process to etch the top silicon layer. A 1.5-μm-thick silica layer is deposited by plasma enhanced chemical vapor deposition (PECVD) as upper-cladding. Grating couplers for TE polarization are employed at the two ends of the input and output ports to couple light into/out of the device with single-mode fibers.

The micrograph of the fabricated device is shown in Fig. 3(a). The coupling lengths are $L_{c1} = L_{c2} = L_{c3} = 5$ μm. $L_a = 24.4$ μm and $L_b = 43.9$ μm are determined by the topology. The blue solid curve in Fig. 3(b) presents the normalized measured transmission spectrum of the fabricated device. 12-dB on-chip insertion loss is introduced by vertical coupling system. A maximum transmission difference of ~ 9 dB is achieved in the transparency peaks between the split resonances. The red dashed curve shows the fitted transmission spectrum. The fitting parameters are: transmission coefficients of the couplers $r_1 = r_2 = r_3 = 0.801$, propagation loss $\alpha = 6.9$ dB/cm, and group index $n_g = 4.3090$.
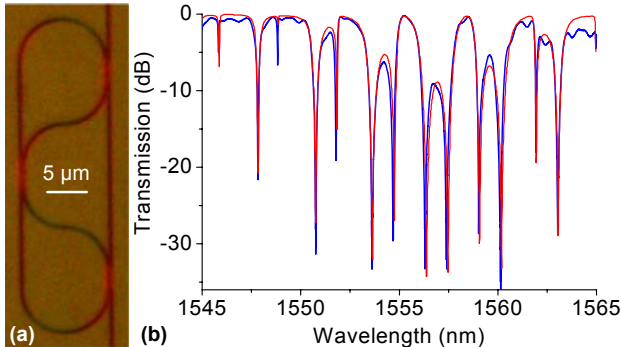

Fig. 3. (a) Micrograph of the fabricated device with $L_{c1} = L_{c2} = L_{c3} = 5$ μm. (b) Measured (blue solid curve) and fitted (red dashed curve) transmission spectra.

As discussed in Section II, there are some non-splitting resonances if r_2 becomes large enough. At these non-splitting resonances with broadened bandwidths, high-order filtering can be realized. Another group of parameters are chosen for demonstration with $L_{c1} = L_{c3} = 10$ μm, $L_{c2} = 6$ μm, $L_a = 29.4$ μm, and $L_b = 44.8$ μm. The micrograph of the fabricated device is shown in Fig. 4(a) and the normalized measured transmission spectrum is provided in Fig. 4(b). Inset shows zoom-in view of the spectrum around 1553.0 nm with flat-bottom filtering function. The 3-dB bandwidth of the dip is ~ 1.23 nm, and the extinction ratio is ~ 28.4 dB. The fitted transmission spectrum is shown by the red dashed curve with the following fitting

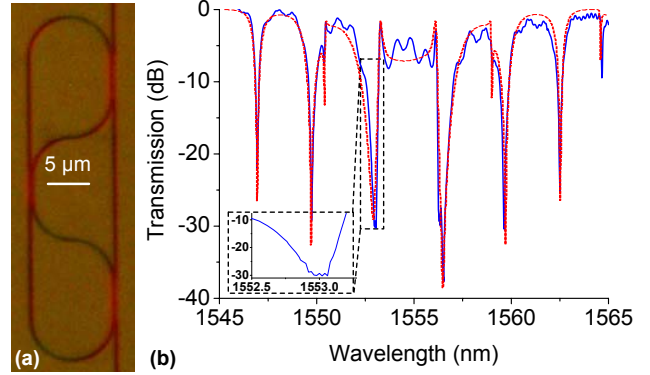parameters: $r_1 = r_3 = 0.580$, $r_2 = 0.771$, propagation loss $\alpha = 6.9$ dB/cm, and group index $n_g = 4.2818$.

Fig. 4. (a) Micrograph of another fabricated device with $L_{c1} = L_{c3} = 10$ μm, and $L_{c2} = 6$ μm. (b) Measured (blue solid curve) and fitted (red dashed curve) transmission spectra. Inset: zoom-in view of the high-order filtering spectrum.

IV. CONCLUSION

We have proposed and experimentally demonstrated a configuration of asymmetrically side-coupled Sagnac loops on a SOI platform. Diverse transmission intensities at split resonances are achieved using a single passive device which provides richer spectrum for signal processing at various wavelengths. The non-splitting resonances with enlarged bandwidths can also be used for high-order filtering.

V. ACKNOWLEDGEMENT

REFERENCES

[1] Q. Li, Z. Zhang, F. Liu, M. Qiu, and Y. Su, "Dense wavelength conversion and multicasting in a resonance-split silicon microring," *Appl. Phys. Lett.*, vol. 93, no. 081113, pp. 1-3, 2008.
[2] Q. Li, Z. Zhang, J. Wang, M. Qiu, and Y. Su, "Fast light in silicon ring resonator with resonance-splitting," *Opt. Exp.*, vol. 17, no. 2, pp. 933-940, 2009.
[3] T. Wang, F. Liu, J. Wang, Y. Tian, Z. Zhang, T. Ye, M. Qiu, and Y. Su, "Pulse delay and advancement in SOI microring resonators with mutual mode coupling," *J. Lightw. Technol.*, vol. 27, no. 21, pp. 4734-4743, 2009.
[4] Z. Zou, L. Zhou, J. Xie, X. Sun, L. Lu, X. Li, and J. Chen, "Tunable two-stage self-coupled optical waveguide (SCOW) resonators," presented at the *OFC*, Paper OTu3C, 2013.
[5] T. Wang, Z. Zhang, F. Liu, T. Ye, J. Wang, Y. Tian, M. Qiu, and Y. Su, "Modeling of quasi-grating sidewall corrugation in SOI microring add-drop filters," *Opt. Commun.*, vol. 282, pp. 3464-3467, 2009.
[6] L. Zhou, T. Ye, and J. Chen, "Waveguide self-coupling based reconfigurable resonance structure for optical filtering and delay," *Opt. Exp.*, vol. 19, no. 9, pp. 8032-8044, 2011.
[7] A. Yariv, "Critical coupling and its control in optical waveguide-ring resonator systems," *IEEE Photon. Technol. Lett.*, vol. 14, no. 4, pp. 483-485, 2002.